

Exploring The Frequency Of Close-In Jovian Planets Around M Dwarfs ¹

Michael Endl, William D. Cochran

McDonald Observatory, The University of Texas at Austin, Austin, TX 78712

mike@astro.as.utexas.edu ; wdc@astro.as.utexas.edu

Martin Kürster

Max-Planck-Institut für Astronomie, Königstuhl 17, Heidelberg, D-69117

kuerster@mpia.de

Diane B. Paulson

NASA Goddard Space Flight Center, Planetary Systems Branch, Greenbelt, MD 20771

Diane.B.Paulson@gsfc.nasa.gov

Robert A. Wittenmyer, Phillip J. MacQueen, Robert G. Tull

McDonald Observatory, The University of Texas at Austin, Austin, TX 78712

robw@astro.as.utexas.edu ; pjm@astro.as.utexas.edu ; rgt@astro.as.utexas.edu

ABSTRACT

We discuss our high precision radial velocity results of a sample of 90 M dwarfs observed with the Hobby-Eberly Telescope and the Harlan J. Smith 2.7 m Telescope at McDonald Observatory, as well as the ESO VLT and the Keck I telescopes, within the context of the overall frequency of Jupiter-mass planetary companions to main sequence stars. None of the stars in our sample show variability indicative of a giant planet in a short period orbit, with $a \leq 1$ AU. We estimate an upper limit of the frequency f of close-in Jovian planets around M dwarfs as $< 1.27\%$ (at the 1σ confidence level). Furthermore, we determine the efficiency of our survey to have noticed planets in circular orbits as 98% for companions with $m \sin i > 3.8 M_{\text{Jup}}$ and $a \leq 0.7$ AU. For eccentric orbits ($e = 0.6$) the survey completeness is 95% for all planets with $m \sin i > 3.5 M_{\text{Jup}}$ and $a \leq 0.7$ AU. Our results point toward a generally lower frequency of close-in Jovian planets for M dwarfs as compared to FGK-type stars. This is an important piece of information for our understanding of the process of planet formation as a function of stellar mass.

Subject headings: stars: late-type — stars: low mass — planetary systems — techniques: radial velocities

1. Introduction

Despite the stunning success of the radial velocity (RV) technique in finding extrasolar planets (e.g. Mayor & Queloz 1995), which resulted in the discovery of more than 160 planetary companions over the past decade, our understanding of planet formation is far from complete. We are especially lacking a general overview of the frequency of planetary companions to stars throughout the entire HR-diagram. Doppler surveys have traditionally targeted bright solar type main sequence stars and it is no big surprise that most planets were found around G-type stars. But, is this entirely a result of an observational bias, or is it a true effect which could lead to a better understanding of the underlying physics of planet formation?

The majority of the stars in the solar neighborhood are M dwarf stars with masses of $0.5 M_{\odot}$ or less (Henry 1998). In order to determine the overall galactic population of planets it is important not to “overlook” the faint and low mass regime of the HR-diagram and to control observational biases in order to arrive at statistically meaningful results. Because of the intrinsic faintness of M dwarfs it is generally more difficult and time consuming to achieve the high quality RV data for the detection of planetary companions. This led to the situation that M dwarfs constitute only small subsets in the target samples of most precision Doppler surveys.

So far, we know of only one M dwarf, GJ 876 (M4 V, $M=0.3 M_{\odot}$), to harbor a planetary system with Jupiter-mass companions (Delfosse et al. 1998; Marcy et al. 1998; Marcy et al. 2001; Benedict et al. 2002). There is the possibility that the giant planet detected by microlensing (Bond et al. 2004) also orbits an M dwarf, but the exact spectral type of the primary lens has not been determined yet. Butler et al. (2004) announced the discovery of

¹Based on data collected with the Hobby-Eberly Telescope, which is operated by McDonald Observatory on behalf of The University of Texas at Austin, the Pennsylvania State University, Stanford University, Ludwig-Maximilians-Universität München, and Georg-August-Universität Göttingen. Also based on observations collected at the European Southern Observatory, Chile (ESO Programmes 65.L-0428, 66.C-0446, 267.C-5700, 68.C-0415, 69.C-0722, 70.C-0044, 71.C-0498, 072.C-0495, 173.C-0606). Additional data were obtained at the W.M.Keck Observatory, which is operated as a scientific partnership among the California Institute of Technology, the University of California, and the National Aeronautics and Space Administration (NASA), as well as with the McDonald Observatory Harlan J. Smith 2.7 m telescope.

a short periodic Neptune mass planet around the M dwarf GJ 436 and Rivera et al. (2005) presented evidence for an extremely low mass ($M \approx 7.5 M_{\text{Earth}}$) third planetary companion to GJ 876. Bonfils et al. (2005b) reported the detection of a Neptune mass companion to the southern M3 V star GJ 581.

Endl et al. (2003) described the dedicated M dwarf survey at the Hobby-Eberly Telescope (HET) which targets exclusively M dwarfs and presented the data of the first year of the survey. This paper now contains three years of RV results from the on-going HET program with the addition of five years of the M dwarf RV results from our planet search program at the ESO Very large Telescope (VLT), as well as data from the McDonald 2.7 m telescope program and from the Keck Hyades survey. We discuss these results and their implications on the total frequency of detectable giant planets along the main sequence.

2. M dwarf radial velocity results

The precise M dwarf RV results we present here originate from four different Doppler surveys: the majority of the data stem from our dedicated M dwarf survey carried out at the HET (Endl et al. 2003), 20 targets in the southern hemisphere are part of our VLT program (Kürster et al. 2003 ; Kürster & Endl 2004) while 6 M dwarfs (GJ 15 A, GJ 411, GJ 412 A, GJ 671, GJ 725 A & B) were monitored as part of our long term survey using the Harlan J. Smith (HJS) 2.7 m telescope at McDonald (e.g. Cochran et al. 1997 ; Hatzes et al. 2003 ; Endl et al. 2004) and 15 M dwarfs were part of the Keck I HIRES survey of the Hyades cluster (Cochran, Hatzes, Paulson 2002 ; Paulson, Cochran, Hatzes 2004).

Targets are selected based on the Gliese catalog of nearby stars (Gliese & Jahreiß 1991) and the *Hipparcos* catalog (Perryman 1997). We choose nearby M dwarfs which are brighter than $V = 12$ in order to obtain high resolution spectra with sufficient signal-to-noise ratios for precise RV measurements (with the exception of a few Hyades targets). In general we excluded M stars from our survey which show strong coronal X-ray emission using the ROSAT All-Sky-Survey data (Hünsch et al. 1999) to minimize additional RV noise due to stellar activity (exceptions again are Hyades stars and Proxima Cen). Unlikely planet hosts like short periodic binaries are also not included in our survey (with the exception of GJ 623). And for the Hyades survey the brightest M dwarfs in the cluster were selected. Because GJ 876 has already known planetary companions we did not include this M dwarf in our program.

Table 1 lists all 90 M dwarfs along with their spectral type, visual magnitude, distance (based on their *Hipparcos* parallax), number of measurements, total RV rms scatter, mean

measurement uncertainty and the duration of monitoring. The M dwarfs included in this study have a mean magnitude of $V = 10.57$ mag, the brightest target has a V magnitude of 7.48 and the faintest star has $V = 12.98$. On average we obtained 16 measurements per target. The mean time coverage of the targets is 1114 days, with 333 days as the shortest monitoring time span and 2980 days as the longest. 1114 days corresponds to the period of an orbit with a semi-major axis of ≈ 1.7 AU for a $0.5 M_{\odot}$ star.

The 82 M dwarfs of the sample which have a *Hipparcos* parallax measurement are located at a mean distance of 16.9 pc. The closest star is GJ 551 (Proxima Cen) with $d = 1.29$ pc and the most distant target with a *Hipparcos* parallax is at a distance of $d = 58.1$ pc (HIP 16548).

Fig. 1 shows the histogram of the total rms scatter of the RV data. The main peak of the distribution is around 6.0 m s^{-1} . The mean RV scatter is 8.3 m s^{-1} with a σ of 3.9 m s^{-1} . There is a small secondary peak containing 6 stars with $\text{rms} > 15.0 \text{ m s}^{-1}$: GJ 436, which has a low mass planetary companion in a short-period orbit (Butler et al. 2004), and 5 young and active Hyades M dwarfs: BD+07 499, HD 286554, HIP 16548, vA 115 & vA 502.

A more detailed description of the RV results for GJ 1, GJ 15 A (binary), GJ 270 (binary), GJ 310 (binary), GJ 551, GJ 623 (binary), GJ 699 (= Barnard’s star), GJ 725 A&B (binary), and GJ 846 (erratum) is given in the Appendix.

None of the M dwarfs surveyed by our programs reveal an increased RV scatter which can be attributed to Keplerian reflex motion caused by a Jovian planetary companion with $P < T_{\text{Survey}}$.

3. M dwarf planet frequency

With this null result in hand, what kind of conclusions can we draw about the frequency of giant planets orbiting M dwarfs? We follow the procedure outlined in the Appendix of Burgasser et al. (2003) and McCarthy & Zuckerman (2004) and estimate the companion frequency f by using the binominal distribution:

$$P_d(f) = f^d(1 - f)^{N-d} \frac{N!}{(N - d)!d!}. \quad (1)$$

$P_d(f)$ is the probability that an ideal survey of N targets will yield a detection rate d , for a true frequency of companions f .

For the estimation of the M dwarf planet frequency we remove GJ 623 from the sample,

as it is a short period binary with an eccentric orbit. Using only the remaining M dwarf sample (number of stars $N = 89$ and detections $d = 0$) we find $f = 0.46^{+0.81}_{-0.46}\%$ (see Fig. 2). The error bar denotes the area of 68% integrated probability (i.e. 1σ confidence). At this confidence level we thus derive an upper limit for f of 1.27%.

3.1. Survey completeness

Of course, no real survey is an ideal survey. We estimate the completeness of our M dwarf survey by using numerical simulations. We start with the null hypothesis that the observed scatter represents the distribution of our measurement errors (i.e. that no additional signal is buried in the data). For each star we then add Keplerian signals to our data (at the times of observation) and compare the resulting new rms scatter with the originally observed value. If the F-test shows a probability of less than 99% that these two variances are drawn from two different samples, the planetary companion corresponding to the input signal is declared as “missed” by our program. For each period and amplitude we compute Keplerian signals at 10 different orbital phases and for eccentric orbits for each phase at 10 different periastron angles. This results in 100 simulated planets per period, amplitude and target. The amplitude of the input signal is increased until a certain overall threshold (e.g. less than 10% or 5% of all planets are missed) is reached.

Fig. 3 displays the survey sensitivity determined by this method for the case of circular orbits with semi-major axes $a = 0.025$ to 1.0 AU. The limits shown in the figure are for 90%, 95%, 98% and 99% survey completeness. To transform the amplitude information into a mass value we adopt a primary mass of $0.5 M_{\odot}$. Note that the mass limits for the planets are conservative upper limits because for less massive stars these companion mass values would be lower. For less massive M dwarfs this diagram would also move inwards (in terms of orbital semi-major axis), because companions around less massive stars orbit closer to the primary at a given orbital period.

Based on these results we find that we have a 95% efficiency to notice all planets with $m \sin i > 2.3 M_{\text{Jup}}$ at $a \leq 0.7$ AU and of 98% for all $m \sin i > 3.9 M_{\text{Jup}}$ companions at these orbital separations. With the exception of a sharp spike up to $7.4 M_{\text{Jup}}$ at $a = 0.61$ AU we are 99% complete for all planets with $m \sin i > 5.1 M_{\text{Jup}}$ at $a \leq 0.7$ AU. For periods close to 1 year ($a \approx 0.8$ AU for a $0.5 M_{\odot}$ star) the efficiency drops rapidly due to the window function: 90% of all planets with $m \sin i > 4.0 M_{\text{Jup}}$ and 95% of all $m \sin i > 6.6 M_{\text{Jup}}$ companions.

Orbital eccentricity decreases the survey sensitivity further, because a Doppler survey can easily miss critical orbital phases of eccentric orbits due to sparse sampling and the star

can thus appear to be RV constant. We repeated the simulations with an orbital eccentricity of $e = 0.6$ (which would include the majority of known extrasolar planets) and the results are displayed in Fig. 4. For orbital separations of $a \leq 0.7$ AU we are 95% complete for planets with $m \sin i > 3.4 M_{\text{Jup}}$ and 98% for $m \sin i > 6.7 M_{\text{Jup}}$. Again, the survey efficiency drops rapidly for periods close to 1 year.

4. Discussion

Marcy et al. (2005) find a frequency of $1.2 \pm 0.2\%$ of “hot Jupiters” with $a < 0.1$ AU around FGK-type stars and according to their Fig.2 a frequency of $2.5 \pm 0.4\%$ of planets with $a < 1$ AU. While the frequency of “hot Jupiters” is still consistent with our results, it appears that there is a difference emerging between the detection rate of Jovian planets with $a < 1$ AU around FGK-type stars and M dwarfs. Also Butler et al. (2004) noted that the combined results from all radial velocity planet search programs, which include M dwarfs in their target samples, point toward an upper limit for f of $< 0.5\%$. Lineweaver & Grether (2003) presented an analysis and extrapolation of the planet frequency for FGK-type stars currently monitored by Doppler surveys. They find that the fraction of detected planets increases from $\approx 3.9 \pm 1\%$ for a survey duration of 2 years to $5.5 \pm 1.5\%$ for a 4 year survey. Again, both values are higher than the upper limit we find. However, our upper limit of 1.27% for M dwarf planets is only valid in the planet mass-separation range, to which our program is most sensitive (with a $> 98 - 99\%$ completeness, see Fig. 3 and Fig. 4). But, also FGK-star surveys are not ideal surveys and they miss a small fraction of planets.

Gaudi et al. (2002) also finds a low frequency for Jupiter-mass companions around M dwarfs in the galactic bulge based on the results of the PLANET microlensing survey. However, one has to bear in mind that the PLANET survey samples a different region of our galaxy and a comparison with the solar neighborhood could be inadequate.

A general observational bias as explanation for a lower M dwarf Jovian planet frequency becomes increasingly unlikely but is not completely ruled out. Doppler surveys of FGK-type stars usually have a higher RV precision than M dwarf programs. The bias introduced by a somewhat lower RV precision for M dwarfs is partly compensated by the fact that the RV amplitudes induced by giant planets around M dwarfs are larger because of the lower mass of the host star and thus easier to detect. Using large aperture telescopes allows us to overcome their intrinsic faintness and to obtain high quality RV data also for these late spectral types. Continuation, improvement and expansion of current M dwarf Doppler surveys is necessary to allow a better determination of the planet frequency around these stars and to perform a more detailed comparison with the results from the FGK-star surveys.

Another issue which could still lead to an unintentional observational bias in our M dwarf sample is stellar metallicity. In recent years, it has become more and more obvious that the frequency of detectable planets is a function of the metal content of the stars included in Doppler surveys (Fischer & Valenti 2005 ; Santos, Israelian, & Mayor 2004). Metal poor stars appear to harbor fewer planets detectable by the RV technique (close in massive planets) than metal rich stars. This could mean that the formation mechanism is somehow linked to the metal content in the protoplanetary disk (at least for the stars included in these surveys). Is it possible that we mostly targeted metal poor M dwarfs and that this is the reason for the observed low planet frequency? Our HET and VLT samples are biased toward inactive and thus presumably older M dwarfs. Thus, it is conceivable that the majority of these M dwarfs are metal poor. A survey including also more active M dwarfs as well as the determination of the metallicities of the targets can solve this issue. Unfortunately, there are no large scale spectroscopic surveys to determine precise metallicities of M dwarfs, although there are efforts under way to find suitable techniques (e.g. Valenti et al. 1998). Woolf & Wallerstein (2005) presented $[\text{Fe}/\text{H}]$ measurements for 35 M and K dwarfs. Three M dwarfs from our sample, GJ 411, GJ 412 A, and GJ 687 are included in their study. They find that GJ 411 and GJ 412 A are metal poor ($[\text{Fe}/\text{H}] \approx -0.4$), while GJ 687 is metal rich ($[\text{Fe}/\text{H}] \approx 0.15$). Iron abundances for three more stars (GJ 15 A, GJ 109, GJ 849) of our sample are estimated by Bonfils et al. (2005a). These authors used visual binaries with M dwarf secondaries to calibrate a photometric method to derive M dwarf metallicities. GJ 15 A ($[\text{Fe}/\text{H}] \approx -0.45$) and GJ 109 ($[\text{Fe}/\text{H}] \approx -0.2$) turn out to be metal poor stars, while GJ 849 ($[\text{Fe}/\text{H}] \approx 0.14$) has a higher than solar iron abundance. So far, four out of six target stars with $[\text{Fe}/\text{H}]$ measurements thus turn out to be metal poor stars. A detailed determination of the metallicity of our sample stars using the method of Bean et al. (2005) is currently in progress. The Hyades M dwarfs are of course young and active stars. They should have a similar metal content as the cluster mean of $[\text{Fe}/\text{H}] = 0.13 \pm 0.01$ (Paulson, Sneden, Cochran 2003). But the small number of M dwarfs included in the overall Hyades sample prevents a meaningful comparison with the planet frequency of earlier type stars in that metallicity range.

How do our observations agree with current models for planet formation? Laughlin, Bodenheimer & Adams (2004) explored the formation of gas giants around M dwarfs within the framework of the core accretion model (e.g. Pollack et al. 1996). These authors conclude that this model has severe problems in forming Jupiter-class planets in the less massive protoplanetary disks of M dwarfs. Also, Ida & Lin (2005) show that close-in Jovian planets should be relatively rare around M dwarfs. Our data confirm so far their theoretical prediction that M dwarfs should harbor fewer gas giant planets. On the other hand, Boss (2006) shows that the gravitational instability model has a higher efficiency in forming giant planets

in less massive M dwarf disks. GJ 876 remains the only unambiguous case of an M dwarf orbited by Jupiter-mass planetary companions despite the accumulation of high quality RV data for more M dwarfs over the past years. So what makes GJ 876 so special? At the moment we can only speculate that GJ 876 had either a more massive disk than other M dwarfs, albeit for unknown reasons, or these planets indeed formed by gravitational instability. As suggested by Boss (2006), M dwarfs could be used as a test ground for competing giant planet formation models.

In the case that orbital migration (e.g. Lin et al. 1996) results in the observed small semi-major axes for many of the planets detected by Doppler surveys, we can pose the question of whether this mechanism might be less efficient for M dwarfs. This would explain the current null detections (again with the exception of GJ 876) because high quality RV data for most M dwarfs do not have sufficient time coverage to find (or exclude) Jupiter-type companions in long periodic orbits. In our sample we do observe RV trends indicating more distant companions, but most of them are quite large and most likely caused by stellar companions. Highly precise astrometric studies using data from the upcoming Space Interferometry Mission (SIM) should allow the detection of planets at large orbital separations around nearby M dwarfs. Firm upper limits from astrometry have been placed by Benedict et al. (1999) on the masses of planetary companions in the period range from 60 to 600 days, orbiting Barnard’s star and Proxima Centauri, using HST Fine Guidance Sensor data. Benedict et al. (2002) succeeded in detecting the astrometric perturbation caused by the outermost planet in the GJ 876 system, and derived a mass for the companion of $1.89 \pm 0.34 M_{\text{Jup}}$.

Despite their lack of close-in Jovian planets, M dwarfs remain attractive targets for current Doppler surveys. Because of their low primary masses the RV amplitude induced by an orbiting companion is higher than for F, G, or K type stars. The discovery of planets with extremely low masses (a few M_{Earth}) using precise radial velocity measurements is feasible in the M dwarf regime (e.g. Kürster et al. 2003). Model calculations (e.g. Wetherill 1996 ; Laughlin et al. 2004) also show no difficulties in forming low mass planets via planetesimal accretion in disks around M dwarfs. Ida & Lin (2005) even predict a higher frequency of icy giant planets with masses comparable to Neptune in short periodic orbits for M dwarfs than for G type stars. The lowest mass extrasolar planet our group has found so far is the fourth companion in the ρ^1 Cnc (G8 V) system (McArthur et al. 2004). The RV semi-amplitude induced by this planet is only 6.7 m s^{-1} and hence a difficult signal to detect. If the same planet ($P = 2.81$ days, $m \sin i = 14.2 M_{\text{Earth}}$) were to orbit a high mass M dwarf ($0.5 M_{\odot}$) the RV semi-amplitude would increase to 10.2 m s^{-1} and for Proxima Centauri (M5 V, $0.12 M_{\odot}$) the signal would be 26.3 m s^{-1} . The discoveries of the short-period Neptunes by Butler et al. (2004) and Bonfils et al. (2005b) and of an additional planet with an extremely low mass of $m \approx 7.5 M_{\text{Earth}}$ in the GJ 876 system (Rivera et al. 2005) further support the notion

that M dwarf stars remain a fruitful and interesting hunting ground for high precision radial velocity surveys. In the future high resolution spectrometers working in the near infrared will be the ideal tools for a more thorough exploration of the red (and low mass) part of the main sequence.

The NASA Kepler mission (Borucki et al. 2003), planned for launch in late 2008, should give much better insight into the true frequency of short-period planets ($P < 1$ year) around M dwarfs, provided a sufficiently large sample of M dwarfs is included in the Kepler target list. M dwarfs are particularly good targets for large photometric transit surveys such as Kepler because their significantly smaller radius than solar-type stars results in a much larger photometric signal for a given planet size.

We thank the anonymous referee for many suggestions which helped to improve the manuscript. We are grateful to the McDonald Observatory Time Allocation Committee and the ESO OPC for generous allocation of observing time. The help and support of the HET staff and especially of the resident astronomers: Matthew Shetrone, Brian Roman, Steven Odewahn and Jeff Mader were crucial for this project. This material is based upon work supported by the National Aeronautics and Space Administration under Grant NNG04G141G. DBP is currently a National Research Council fellow working at NASA’s Goddard Space Flight Center. This research has made use of the SIMBAD database, operated at CDS, Strasbourg, France.

5. APPENDIX

5.1. Individual results

5.1.1. Secular RV accelerations: GJ 1, GJ 411, GJ 551 and GJ 699

For these 4 nearby M dwarfs we subtract from our data the expected secular acceleration of the RV caused by their proximity and/or large space motion. A detailed discussion of this effect and its measurement using our data for Barnard’s star (GJ 699) is given by Kürster et al. (2003). The value of the secular accelerations for GJ 1 is $3.7 \text{ m s}^{-1} \text{ yr}^{-1}$, for GJ 411: $1.35 \text{ m s}^{-1} \text{ yr}^{-1}$, for GJ 551 (Proxima Cen): $0.45 \text{ m s}^{-1} \text{ yr}^{-1}$, and for GJ 699: $4.5 \text{ m s}^{-1} \text{ yr}^{-1}$.

5.1.2. GJ 15 A, GJ 270, GJ 310 & GJ 725 A&B

GJ 15 A (= HIP 1475 = HD 1326 A) is the primary of an M dwarf binary system with an angular separation to component B of 36 arcseconds. We detect a linear RV trend of $+1.45 \pm 0.40 \text{ m s}^{-1} \text{ yr}^{-1}$ ($\chi_{\text{red}}^2 = 1.47$, dof = 27), which might be part of the long period orbit of the primary in this system. However, part of this RV trend is also the expected secular acceleration of $0.7 \text{ m s}^{-1} \text{ yr}^{-1}$.

The M0 V star GJ 270 (= HIP 35495 = G 87-33 = BD+33 1505) also exhibits a linear RV acceleration. We fit a trend of $+171.4 \pm 2.2 \text{ m s}^{-1} \text{ yr}^{-1}$ with a χ_{red}^2 of 1.42 (dof = 26). The residual rms scatter of the RV measurements around this linear RV trend is 12.0 m s^{-1} . This trend is presumably caused by a previously unknown stellar companion in a long periodic orbit. The *Hipparcos* data for this star do not detect any astrometric perturbation which also points toward a long period of the binary.

For GJ 310 (= HIP 42220 = G 234-38 = BD+67 552) we have almost exactly the same situation as for GJ 270. We detect a linear RV trend of similar magnitude. But in this case a stellar secondary with a long period of ≈ 24 yrs (Heintz & Cantor 1994) is already known. This companion is very likely the cause of the observed RV trend. We fit a linear RV trend of $+199.0 \pm 0.6 \text{ m s}^{-1} \text{ yr}^{-1}$ with $\chi_{\text{red}}^2 = 10.6$ (dof = 36). Because the angular separation of the two components is only 0.55 arcsecs, we cannot rule out that spectral contamination by the secondary is the cause of the high χ_{red}^2 value and large residual scatter of 13.7 m s^{-1} .

GJ 725 is a known binary consisting of 2 M dwarfs at an angular separation of 13.3 arcseconds (projected minimum separation is ≈ 47 AU). For component A we find a linear RV trend of $+6.99 \pm 0.86 \text{ m s}^{-1} \text{ yr}^{-1}$ ($\chi_{\text{red}}^2 = 0.9$, dof = 21) and for component B of $-4.99 \pm 1.12 \text{ m s}^{-1} \text{ yr}^{-1}$ ($\chi_{\text{red}}^2 = 0.67$, dof = 18). Because the trends have opposite signs it is very probable that in both cases we see a small section of the binary orbit.

5.1.3. GJ 623

For the known binary GJ 623 (Lippincott & Borgman 1978) we find an orbital solution yielding the following parameters: $P = 1291.8 \pm 15.9$ days, $T_{\text{periastron}} = 2451402.8 \pm 29.7$, $K = 2198.0 \pm 14.7 \text{ m s}^{-1}$, $e = 0.618 \pm 0.016$, $\omega = 245.7 \pm 1.2$, close to the latest published values by Nidever et al. (2002). The residual rms scatter around this orbit is $\sigma = 7.7 \text{ m s}^{-1}$ ($\chi_{\text{red}}^2 = 0.6$, dof = 16). The HET data along with the Keplerian orbital solution are displayed in Fig.5. The high eccentricity and short period of the binary orbit makes GJ 623 A an unlikely host star for a close-in planetary companion (but see Konacki 2005 for an example of a hot Jupiter in a tight binary system). Assuming a stellar mass of $0.3 \pm 0.1 M_{\odot}$ we derive a minimum

mass value for the secondary of $m \sin i = 41.5 \pm 9.0 \text{ M}_{\text{Jup}}$. A combination of these RV data with HST/FGS astrometry and other RV data sets will allow a further refinement of the orbit and will result in an accurate mass for the secondary companion (Benedict et al., in prep.).

5.1.4. Erratum: GJ 864

In Endl et al. (2003) we discussed our results for GJ 864, which showed a large linear RV trend of $\approx -2.0 \text{ km s}^{-1} \text{ yr}^{-1}$, possibly due to a previously unknown stellar companion. Unfortunately, shortly after publication we found an error in the coordinate entry for this target which introduced a systematic error into the correction to the barycenter of the solar system. After correction of this mistake we find a much smaller linear RV trend of $-32.3 \pm 2.4 \text{ m s}^{-1} \text{ yr}^{-1}$ ($\chi^2_{\text{red}} = 0.97$, dof = 25). The residual scatter around this trend is 10.4 m s^{-1} almost identical to our average uncertainty of 10.7 m s^{-1} . The classification of GJ 864 as RV constant star using the less precise CORAVEL data by Tokovinin (1992) is correct, considering the much shallower trend now. The companion causing this linear trend has probably a period far exceeding our 999 days of monitoring.

REFERENCES

- Bean, J.L., Benedict, G.F., Endl, M., & Sneden, C. 2005, AAS, 207, 6818
- Benedict, G.F., McArthur, B., Chappell, D.W., Nelan, E., et al. 1999, AJ, 118, 1068
- Benedict, G.F., McArthur, B.E., Forveille, T., Delfosse, X., et al. 2002, ApJ, 581, L115
- Bond, I.A., Udalski, A., Jaroszynski, M., et al. 2004, A&A, 606, L155
- Bonfils, X., Delfosse, X., Udry, S., Santos, N.C., et al. 2005a, A&A, 442, 635
- Bonfils, X., Forveille, T., Delfosse, X., Udry, S., et al. 2005b, A&A, 443, L15
- Borucki, W.J., Koch, D.G., Basri, G.B., Caldwell, D.A., et al. 2003, ASP Conf.Ser., 294, 427
- Boss, A. P. 2006, ApJ, accepted
- Burgasser, A.J., Kirkpatrick, J.D., Reid, N.I., Brown, M.E., Miskay, C.L., & Gizis, J.E. 2003, ApJ, 586, 512
- Butler, R.P., Vogt, S.S., Marcy, G.W., et al. 2004, ApJ, 617, 580

- Cochran, W.D., Hatzes, A.P., Butler, R.P., & Marcy, G.W. 1997, *ApJ*, 483, 457
- Cochran, W.D., Hatzes, A.P., & Paulson, D.B. 2002, *AJ*, 124, 565
- Delfosse, X., Forveille, T., Mayor, M., Perrier, C., Naef, D., & Queloz, D. 1998, *A&A*, 338, L67
- Endl, M., Cochran, W.D., Tull, R.G., & MacQueen, P.J. 2003, *AJ*, 126, 3099
- Endl, M., Hatzes, A.P., Cochran, W.D., McArthur, B., et al. 2004, *ApJ*, 611, 1121
- Fischer, D.A., & Valenti, J.A. 2005, *ApJ*, 622, 1102
- Gaudi, B.S., Albrow, M.D., An, J., Beaulieu, J.-P., et al. 2002, *ApJ*, 566 463
- Gliese, W., & Jahreiß, H. 1991, Preliminary Version of the Third Catalogue of Nearby Stars, Astronomical Data Center CD-ROM
- Hatzes, A.P., Cochran, W.D., Endl, M., McArthur, B., et al. 2003, *ApJ*, 599, 1383
- Heintz, W.D., & Cantor, B.A. 1994, *PASP*, 106, 363
- Henry, T.J. 1998, *ASP Conf. Proc.* Vol. 134, 28
- Hünsch, M., Schmitt, J.H.M.M., Sterzik, M.F., & Voges, W. 1999, *A&ASS*, 135, 319
- Ida, S., & Lin, D.N.C. 2005, *ApJ*, 626, 1045
- Konacki, M. 2005, *Nature*, 436, 230
- Kürster, M., & Endl, M. 2004, *ASP Conf. Proc.* Vol. 321, 84
- Kürster, M., Endl, M., Rouesnel, F., Els, S. et al. 2003, *A&A*, 403, 1077
- Laughlin, G., Bodenheimer, P., & Adams, F.C. 2004, *ApJ*, 612, L73
- Lin, D.N.C., Bodenheimer, P., & Richardson, D.C. 1996, *Nature*, 380, 606
- Lineweaver, C.H., & Grether, D. 2003, *ApJ*, 598, 1350
- Lippincott, S. L., & Borgman, E. R. 1978, *PASP*, 90, 226
- Marcy, G.W., Butler, R.P., Fischer, D., Vogt, S.S., Wright, J.T., Tinney, C.G. & Jones, H.R.A. 2005, *PTThPS*, 158, 24

- Marcy, G.W., Butler, R.P., Fischer, D., Vogt, S.S., Lissauer, J.J., & Rivera, E.J. 2001, *ApJ*, 556, 296
- Marcy, G.W., Butler, R.P., Vogt, S.S., Fischer, D., & Lissauer, J.J. 1998, *ApJ*, 505, L147
- Mayor, M., & Queloz, D., 1995, *Nature*, 378, 355
- McArthur, B.E., Endl, M., Cochran, W.D., Benedict, G.F., et al. 2004, *ApJ*, 614, L81
- McCarthy, C., & Zuckerman, B. 2004, *AJ*, 127, 2871
- Nidever, D. L., Marcy, G. W., Butler, R. P., Fischer, D. A., & Vogt, S. S. 2002, *ApJS*, 141, 503
- Paulson, D.B., Sneden, C., & Cochran, W.D. 2003, *AJ*, 125, 3185
- Paulson, D.B., Cochran, W.D., & Hatzes, A.P. 2004, *AJ*, 127, 3579
- Perryman, M. A. C., ed. 1997, *The Hipparcos and Tycho Catalogues* (ESA SP-1200; Noordwijk: ESA)
- Pollack, J.B., Hubickyj, O., Bodenheimer, P., Lissauer, J.J., Podolak, M., & Greenzweig, Y. 1996, *Icarus*, 124, 62
- Rivera, E., Lissauer, J., Butler, R.P., Marcy, G.W., Vogt, S., Fischer, D.A., Brown, T., & Laughlin, G. 2005, *ApJ*, 634, 625
- Santos, N.C., Israelian, G., & Mayor, M. 2004, *A&A*, 415, 1153
- Tokovinin, A.A. 1992, *A&A*, 256, 121
- Valenti, J.A., Piskunov, N., & Johns-Krull, C.M. 1998, *ApJ*, 498, 851
- Wetherill, G. W. 1996, *Icarus*, 119, 219
- Wolf, V. M., & Wallerstein, G. 2005, *MNRAS*, 356, 963

Table 1. The sample of 90 M dwarfs surveyed with the HET, ESO VLT, HJS 2.7 m and Keck telescopes. Spectral type, visual magnitude (V), distance (d), number of measurements (N), total RV scatter (σ), average internal measurement error ($\bar{\sigma}_{\text{int}}$) and duration of monitoring (ΔT) are given.

Star	HIP	Sp.T.	V [mag]	d [pc]	N	σ [m s ⁻¹]	$\bar{\sigma}_{\text{int}}$ [m s ⁻¹]	ΔT [days]	Survey
GJ 1 ⁽¹⁾	439	M1.5 V	8.57	4.36	15	2.6	2.6	1743	VLT
GJ 2	428	M2 V	9.93	11.5	9	5.2	5.1	721	HET
GJ 15 A ⁽²⁾	1475	M2 V	8.08	3.6	29	5.7	4.9	2680	HJS 2.7 m
GJ 1009	1734	M1.5 V	11.16	18.2	11	6.1	3.3	824	VLT
GJ 27.1	3143	M0.5 V	11.42	22.9	18	6.7	4.7	1443	VLT
GJ 38	4012	M2 V	10.67	18.4	9	6.3	6.5	487	HET
GJ 87	10279	M2.5 V	10.06	10.4	17	8.9	7.3	1209	HET
GJ 96	11048	M1.5 V	9.41	11.9	17	6.8	5.1	386	HET
GJ 109	12781	M3.5 V	10.57	7.6	6	6.4	11.6	388	HET
GJ 118	13389	M2.5 V	10.7	11.5	19	5.1	5.9	1769	VLT
GJ 155.1	17743	M1 V	11.04	17.4	6	7.1	16.8	770	HET
GJ 160.2	19165	M0 V	9.69	23.5	14	7.9	6.3	1451	VLT
GJ 162	19337	M1 V	10.18	13.7	8	7.1	7.7	381	HET
GJ 176	21932	M2.5 V	9.98	9.4	10	5.8	7.8	420	HET
GJ 179	22627	M4 V	11.98	12.1	9	13.9	18.6	422	HET
GJ 180	22762	M2 V	12.5	12.4	13	3.7	3.0	1453	VLT
GJ 181	23147	M2 V	9.78	16.5	7	7.4	4.9	472	HET
GJ 184	23518	M0 V	9.93	14.0	8	2.8	4.3	796	HET
GJ 192	24284	M3.5 V	10.76	12.7	10	9.4	11.8	448	HET
GJ 3352	26113	M3 V	11.07	26.6	14	10.9	13.1	772	HET
GJ 229 A	29295	M2 V	8.14	5.77	22	4.9	3.0	1780	VLT
GJ 251.1	33241	M1.5 V	10.55	48.5	18	9.1	10.1	674	HET
GJ 270 ⁽²⁾	35495	M0 V	10.07	19.8	28	12.0	11.0	1120	HET
GJ 272	35821	M2 V	10.53	16.2	22	9.5	11.0	1099	HET
GJ 277.1	36834	M0 V	10.49	11.5	14	7.2	13.7	403	HET
GJ 281	37288	M0 V	9.61	14.9	11	8.9	5.0	734	HET
GJ 289	38082	M2 V	11.46	14.1	11	8.2	10.3	413	HET
GJ 308.1	41689	M0 V	10.33	19.1	33	10.5	10.3	716	HET
GJ 310 ⁽²⁾	42220	M1 V	9.30	13.9	38	13.7	4.1	1104	HET
GJ 328	43790	M1 V	9.99	20.0	11	11.6	5.2	442	HET
GJ 353	46769	M2 V	10.19	13.5	11	7.5	15.1	408	HET
GJ 357	47103	M2.5 V	10.85	8.98	18	3.7	2.5	1221	VLT
GJ 378	49189	M2 V	10.07	14.9	6	5.2	5.7	747	HET
GJ 411 ⁽¹⁾	54035	M2 V	7.48	2.5	24	5.6	4.5	2536	HJS 2.7 m
GJ 412 A	54211	M2 V	8.68	4.8	23	6.9	7.1	1826	HJS 2.7 m
GJ 2085	55625	M1 V	11.18	21.2	13	12.1	17.9	407	HET
GJ 430.1	56238	M1 V	10.30	16.2	21	10.8	11.7	460	HET
GJ 433	56528	M1.5 V	9.79	9.04	41	4.3	3.6	1938	VLT
GJ 436 ⁽³⁾	57087	M2.5 V	10.67	10.2	57	16.6	14.5	1245	HET
Wolf 9381	58114	M1.5 V	11.50	27.9	14	13.6	18.1	386	HET
GJ 1170	64880	M2 V	11.29	21.6	7	6.8	13.2	353	HET
GJ 510	65520	M1 V	11.05	16.3	15	5.1	3.7	423	VLT
GJ 535	68337	M0 V	9.03	23.8	8	6.8	3.0	769	HET
GJ 551 ⁽¹⁾	70890	M5.5 V	11.05	1.29	69	3.6	2.3	1886	VLT
GJ 552	70865	M2.5 V	10.68	14.3	9	4.4	6.2	769	HET

Table 1—Continued

Star	HIP	Sp.T.	V [mag]	d [pc]	N	σ [m s ⁻¹]	$\bar{\sigma}_{\text{int}}$ [m s ⁻¹]	ΔT [days]	Survey
GJ 563.1	72387	M2 V	9.71	24.2	10	10.9	8.0	767	HET
GJ 618.1	80053	M2 V	10.70	30.3	7	6.8	9.6	440	HET
GJ 623 ⁽⁴⁾	80346	M3 V	10.28	8.0	22	7.7	10.6	892	HET
GJ 637	82256	M0.5 V	11.36	15.9	17	6.4	3.8	1099	VLT
GJ 655	83762	M3 V	11.61	13.5	40	13.4	22.3	1178	HET
GJ 2128	84521	M3.5 V	11.49	14.9	9	7.4	15.9	736	HET
GJ 671	84790	M3 V	11.37	12.3	12	10.1	14.1	742	HET
GJ 682	86214	M3.5 V	10.96	5.04	17	4.3	2.4	1050	VLT
GJ 687	86162	M3.5 V	9.18	4.5	25	9.9	6.5	2514	HJS 2.7 m
GJ 699 ⁽¹⁾	87937	M4 V	9.53	1.8	70	3.4	2.7	1967	VLT
GJ 709	89560	M0 V	10.28	17.1	8	8.8	12.5	427	HET
GJ 4070	91699	M3 V	11.27	11.3	10	6.6	16.4	822	HET
GJ 725 A ⁽²⁾	91768	M3 V	8.91	3.57	23	7.4	8.1	2588	HJS 2.7 m
GJ 725 B ⁽²⁾	91772	M3.5 V	9.69	3.52	20	7.1	9.4	2588	HJS 2.7 m
GJ 730	92417	M1.5 V	10.74	21.8	18	13.3	12.7	822	HET
GJ 731	92573	M1.5 V	10.15	15.6	8	8.2	5.9	852	HET
GJ 739	93206	M2 V	11.14	13.9	19	4.6	3.3	1062	VLT
GJ 817	104059	M1 V	11.48	19.1	20	4.9	4.0	1139	VLT
GJ 821	104432	M1 V	10.87	12.1	31	5.3	3.8	1155	VLT
GJ 828.1	105885	M1 V	10.52	28.6	9	11.3	13.4	425	HET
GJ 839	108092	M1 V	10.35	23.2	11	9.0	6.9	722	HET
GJ 846	108782	M0.5 V	9.18	10.3	6	2.9	4.2	352	HET
GJ 849	109388	M3.5 V	10.37	8.8	7	8.8	10.3	657	HET
GJ 855	110534	M0.5 V	10.74	19.4	17	5.7	4.6	1152	VLT
GJ 864 ⁽²⁾	111571	M1 V	10.01	17.5	27	10.4	10.7	999	HET
GJ 891	114411	M2 V	12.2	15.7	16	5.5	4.0	1768	VLT
GJ 894.1	115058	M0.5 V	10.90	24.3	7	8.4	13.0	361	HET
GJ 895	115562	M2 V	10.04	13.1	10	9.2	6.9	788	HET
GJ 899	116317	M4 V	11.17	14.0	6	4.0	12.2	333	HET
GJ 911	117886	M0 V	10.88	24.7	11	7.8	5.4	834	VLT
BD+07 499	15563	M0 V	9.77	29.3	12	18.4	5.1	2291	KECK
HD 285590	19862	M2 V	11.20	32.1	9	7.0	4.8	2291	KECK
HD 286363	18322	M0 V	10.15	37.8	10	13.4	4.9	1863	KECK
HD 286554	19316	M0 V	11.37	40.2	9	18.7	7.0	1864	KECK
HIP 15720	15720	M0 V	11.12	33.6	10	8.8	7.5	1896	KECK
HIP 16548	16548	M0 V	12.01	58.1	9	17.5	9.5	1864	KECK
HIP 17766	17766	M1 V	10.93	41.6	9	6.4	6.5	1751	KECK
vA 115 ⁽⁵⁾	M1 V	12.98	...	9	19.3	12.9	1864	KECK
vA 146 ⁽⁵⁾	M1 V	11.98	...	7	8.5	7.0	1864	KECK
vA 383 ⁽⁵⁾	M1 V	12.24	...	6	11.4	6.9	1081	KECK
vA 502 ⁽⁵⁾	M1 V	11.95	...	9	20.2	10.4	1836	KECK
vA 731 ⁽⁵⁾	M0 V	12.83	...	5	5.6	6.4	1081	KECK
Melotte 25 303 ⁽⁵⁾	M0 V	11.51	...	6	5.8	5.4	1398	KECK
Melotte 25 332 ⁽⁵⁾	M0 V	11.53	...	7	10.2	6.8	1721	KECK
Melotte 25 348 ⁽⁵⁾	M0 V	11.39	...	5	5.2	5.4	1512	KECK

Table 1—Continued

Star	HIP	Sp.T.	V [mag]	d [pc]	N	σ [m s ⁻¹]	$\bar{\sigma}_{\text{int}}$ [m s ⁻¹]	ΔT [days]	Survey
------	-----	-------	------------	-----------	---	----------------------------------	---	----------------------	--------

¹secular acceleration of the RV subtracted, see Appendix

²inear RV trend subtracted, see Appendix

³GJ 436: $P = 2.64$ days ; Butler et al. (2004)

⁴GJ 623: binary orbit subtracted, see Appendix

⁵No *Hipparcos* data

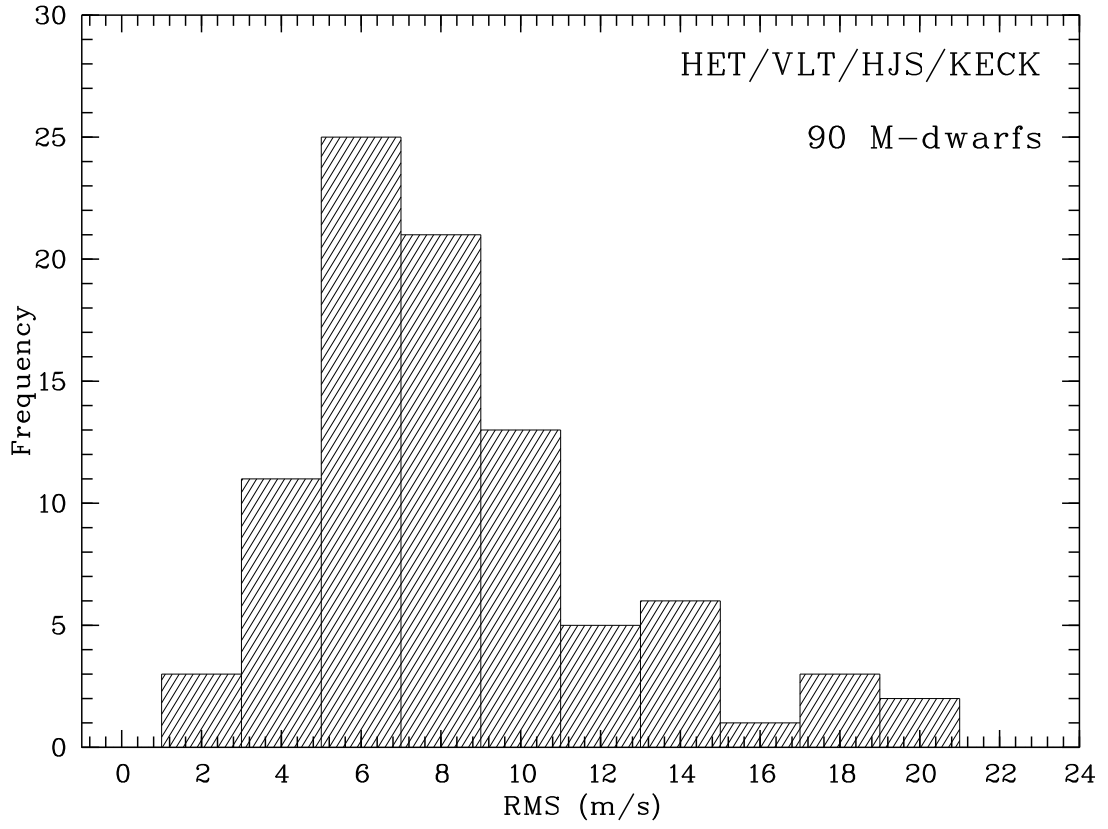


Fig. 1.— Histogram of the total RMS scatter for the 90 M-dwarfs in the sample observed with the HET, VLT, HJS and Keck telescopes. The mean value of this distribution is 8.3 m s^{-1} with a σ of 3.9 m s^{-1} .

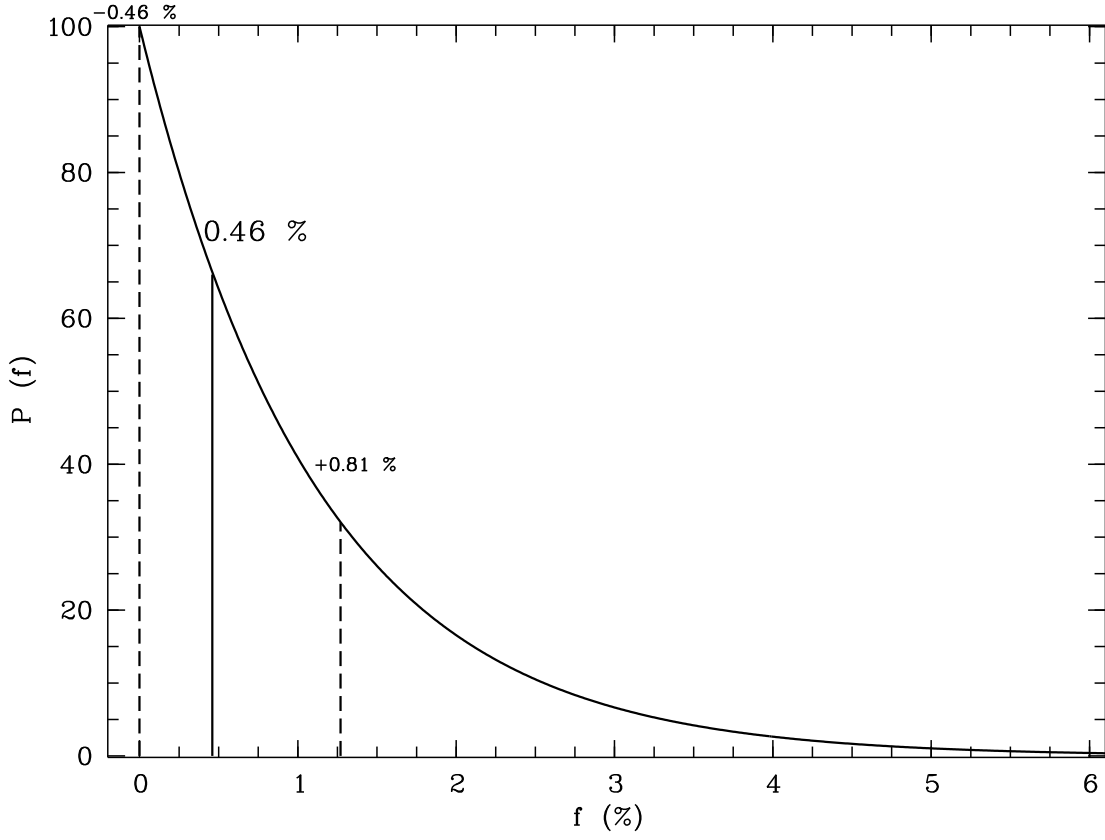


Fig. 2.— Probability function $P(f)$ for the true companion frequency f based on all our M dwarf data (HET, VLT, HJS, and KECK: $N = 89$ stars) and $d = 0$ detections. We find $f = 0.46^{+0.81}_{-0.46}\%$. The dashed lines delimit the area of 68% integrated probability ($\approx 1\sigma$ Gaussian error).

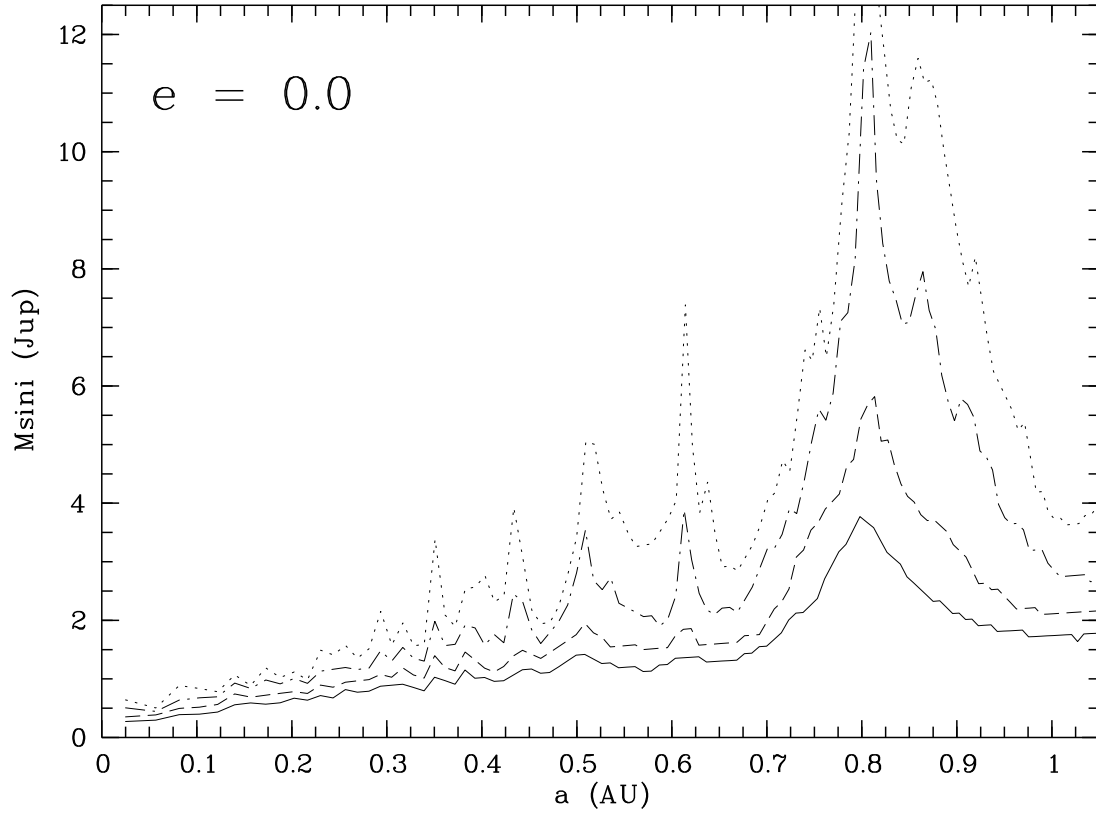


Fig. 3.— Estimated survey completeness for planets in circular orbits. The lines represent 90% success rate (solid line), 95% (dashed line), 98% (dash-dotted line) and 99% (dotted line).

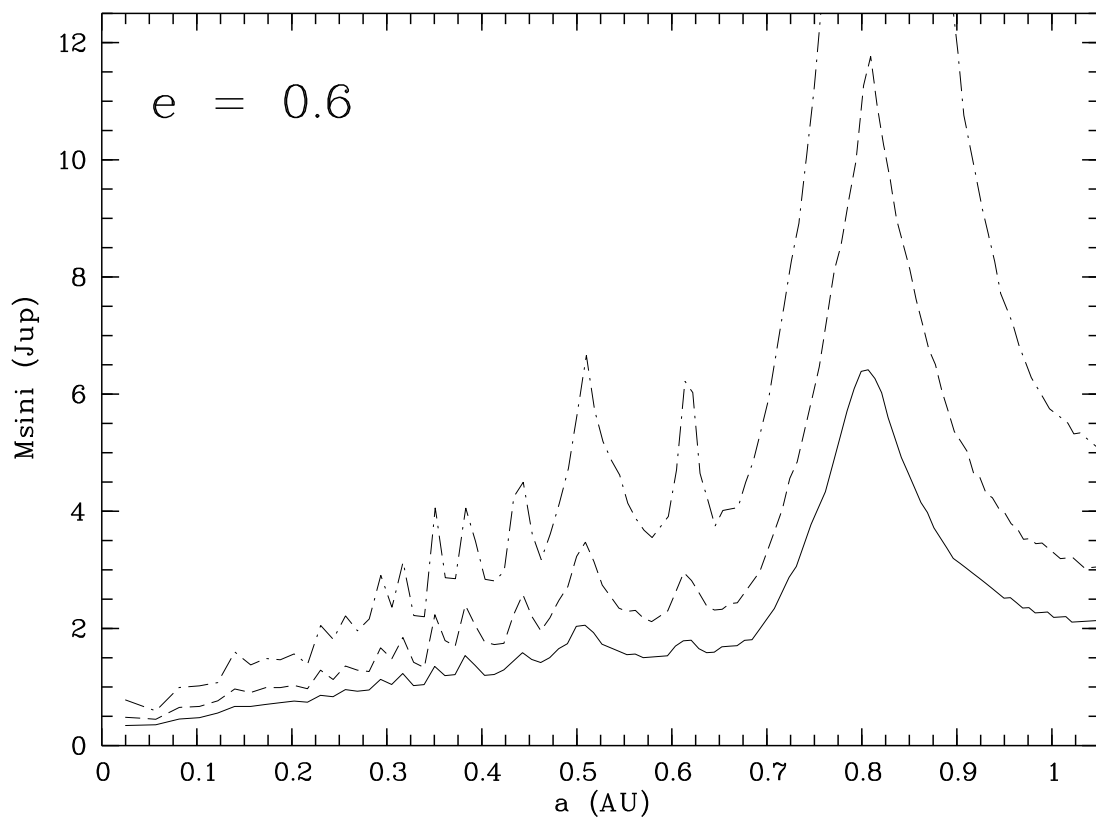


Fig. 4.— Estimated survey completeness for planets in eccentric orbits with $e = 0.6$. The lines represent 90% success rate (solid line), 95% (dashed line) and 98% (dash-dotted line).

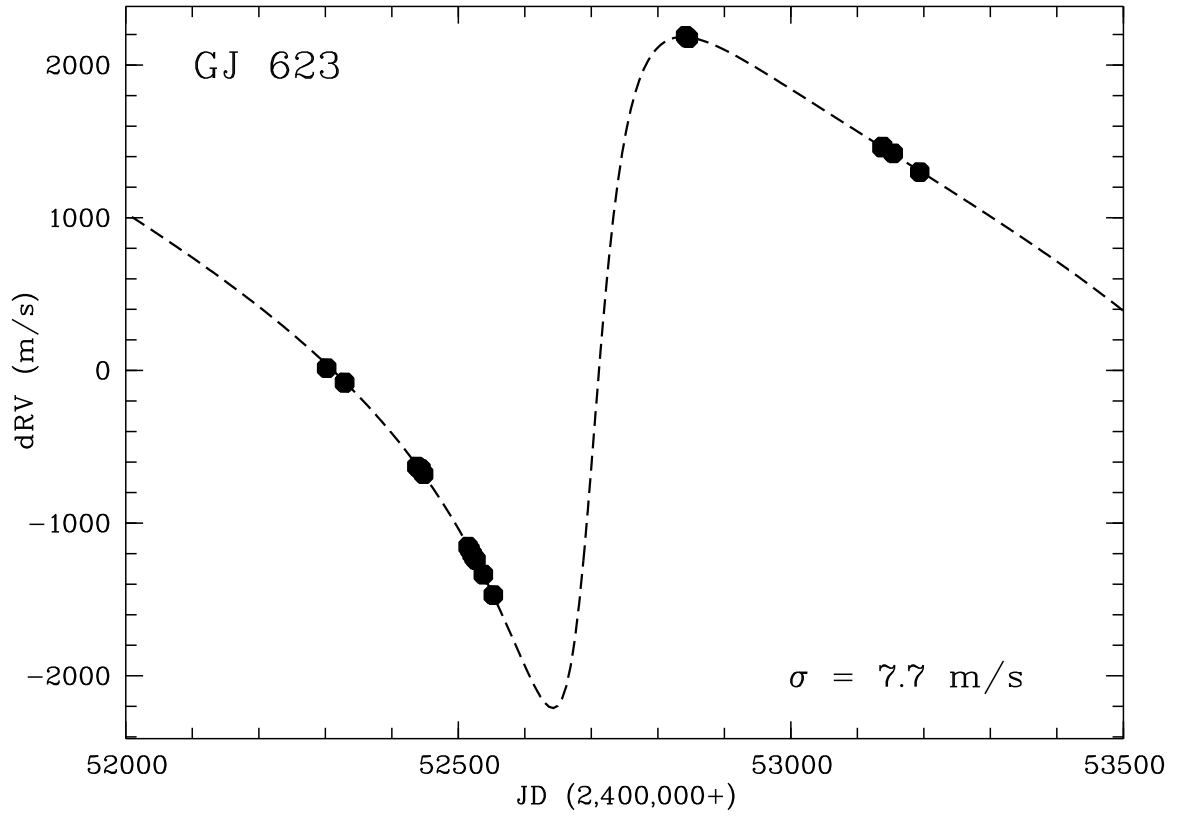


Fig. 5.— HET RV data of GJ 623 (filled circles) with the best-fit Keplerian orbital solution (dashed line) for the binary over-plotted.